

Transition Metals Doping Effects on Non-Linear Optical Properties of $\text{Be}_{12}\text{O}_{12}$ Nano-Cluster: A DFT Study

Ali Raof Toosi and Hamid Reza Shamlouei*

Physical Chemistry Group, Department of Chemistry, Lorestan University, Khorram Abad, Lorestan, Iran

*Corresponding author: Shamlouei HR, Department of Chemistry, Lorestan University, Khorram Abad, Lorestan, I.R. Iran, Tel: 986633120618; E-mail: shamlouei.ha@lu.ac.ir

Received: July 09, 2017; Accepted: July 31, 2017; Published: August 09, 2017

Abstract

Investigation about the effect of transition metal doping on structural, electronic, energetic, linear and nonlinear optical properties of $\text{Be}_{12}\text{O}_{12}$ nanocluster is the subject of this research. Results indicated that transition metals doping process leads to narrowing the energy gap (E_g) of them. Evidently the dipole moment and polarizability value of $\text{Be}_{12}\text{O}_{12}$ nanocluster increases because of that transition metals doping. The first hyperpolarizability value dramatically increases as substitute a magnesium atom with a transition metal atom. Among the transition metal atom doped nanocage, scandium has the largest first hyperpolarizability value ($\beta_0 \approx 4953$ au). Also two-level model indicated that first hyperpolarizability has severe dependence to excitation energies. The result of TD-DFT calculation indicates that the β_0 has similar behavior as β_2 which confirm the results of β_0 obtained by ab initio calculation.

Keywords: Transition metals; $\text{Be}_{12}\text{O}_{12}$; Doping; NLO; Nanocage; First hyperpolarizability

Introduction

Due to the great applications, compounds with high nonlinear optical properties in the fields of optoelectronic and photonic devices, especially generation of optical harmonics, the scientists were attracted to investigate about material with high NLO properties [1-7]. There are many effective agents for enhancing the NLO properties such as: Electron donor and recipient groups, establishment of electron π , doping atom and etc. in original molecule [8-11]. Discovery of carbon nanotube [12] made a significant revolution in science and technology of nanomaterials. Scientists became interested to explore their new types of nanomaterial with unique properties and different functionalities. It has been shown that homologues of fullerene molecules have excellent applications in electronic devices, imaging materials, magnetic recording, and environmental processes; so, their investigation will be very interesting [13-16]. Theoretically, it is shown that, between different types of $(\text{XY})_n$ structures, the nanocages with the general formula of $(\text{XY})_{12}$ have the most stable clusters [17-20] which employ in various application. To enhance the NLO properties of $\text{X}_{12}\text{Y}_{12}$ nanoclusters many efforts were done [21,22]. Recently, the effect of transition metals atoms doping on geometric, electronic, linear and nonlinear optical properties of $\text{Mg}_{12}\text{O}_{12}$ nanocage was investigated and it was shown that the first hyperpolarizability of $\text{Mg}_{12}\text{O}_{12}$ nanoclusters significantly enhanced through doping with transition metal atoms [23]. In present study, in the similar way, the effect of transition metal doping on $\text{Be}_{12}\text{O}_{12}$

Citation: Toosi AR, Shamlouei HR. Transition Metals Doping Effects on Non-Linear Optical Properties of $\text{Be}_{12}\text{O}_{12}$ Nano-Cluster: A DFT Study. Phys Chem Ind J. 2017;S1:103. © 2017 Trade Science Inc.

nanocluster was studied. Calculation of the energies of the singlet excited states using time-dependent density functional (TD-DFT) method is the benefit of this research in comparison of previous research.

Computational Details

In this paper, all theoretical computations were done using density functional theory (DFT) with Gaussian 09 package [24]. All optimization calculations for considered nanocluster structures $Be_{12}O_{12}$ and $Be_{11}XO_{12}$ (X = transition metals atom) in ground state and excited state were calculated by B_3LYP method in 6-31+g(d) basis set. Vertical energies of the singlet excited states were calculated using time-dependent density functional (TD-DFT) method at the $B_3LYP/6-31+g(d)$ level. The values of $\langle S^2 \rangle$ are 0.750 for a pure doublet and 0 for pure singlet systems, after spin annihilation. Recently has been developed for long-range interaction and charge transfer systems, a new density functional CAM- B_3LYP [25,26] that can be useful for (hyper) polarizabilities calculations [27,28] and for considered nanocluster structures linear and non-linear optic properties and hyperpolarization were investigated.

We used CAM- B_3LYP method in 6-31+g(d) level for determination of first hyperpolarizability. The electronic properties of the considered nanocluster such as: the values of energies of HOMO (the highest occupied molecular orbital; E_{HOMO}), LUMO (lowest unoccupied molecular orbital; E_{LUMO}) and the energy gap (E_g) difference of between HOMO and LUMO levels as a critical parameter to determine molecular electrical transport properties investigated through their density of states (DOS) spectra obtained from GaussSum program [29].

The energy gap (E_g) is given as Eq. 1

$$E_g = E_{(HOMO)} - E_{(LUMO)} \quad (1)$$

Where E_g is the energy gap, E_{HOMO} and E_{LUMO} are the values of energie of the highest and the lowest occupied molecular orbitals, respectively (in Ev).

The energy of an uncharged liner molecule in a weak and homogeneous external electric field can be defined as Eq. (2) [30,31].

$$E = E_0 - \mu_a F_a - 1/2 \alpha_{\alpha\beta} F_\alpha F_\beta - 1/6 \beta_{\alpha\beta\gamma} F_\alpha F_\beta F_\gamma - \dots \quad (2)$$

Where E_0 is energy of system in zero electric field and F_α is the electric field component alongside α direction. μ_α , $\alpha_{\alpha\beta}$ and $\beta_{\alpha\beta\gamma}$ are the components of dipole moment, polarizability, and the first hyperpolarizability tensor.

The polarizability (α), first hyperpolarizability (β) and tensor components of first hyperpolarizability (β_{ijk}) are noted as: [32,33]

$$\alpha = 1/3(\alpha_{xx} + \alpha_{yy} + \alpha_{zz}) \quad (3)$$

$$\beta_0 = (\beta_x^2 + \beta_y^2 + \beta_z^2)^{1/2} \quad (4)$$

$$\text{In which } \beta_i = 3/5 (\beta_{iii} + \beta_{ijj} + \beta_{ikk}) \quad i, j, k=x, y, z \quad (5)$$

Where β_{ijk} ($i, j, k = x, y, z$) are tensor components of first hyperpolarizability.

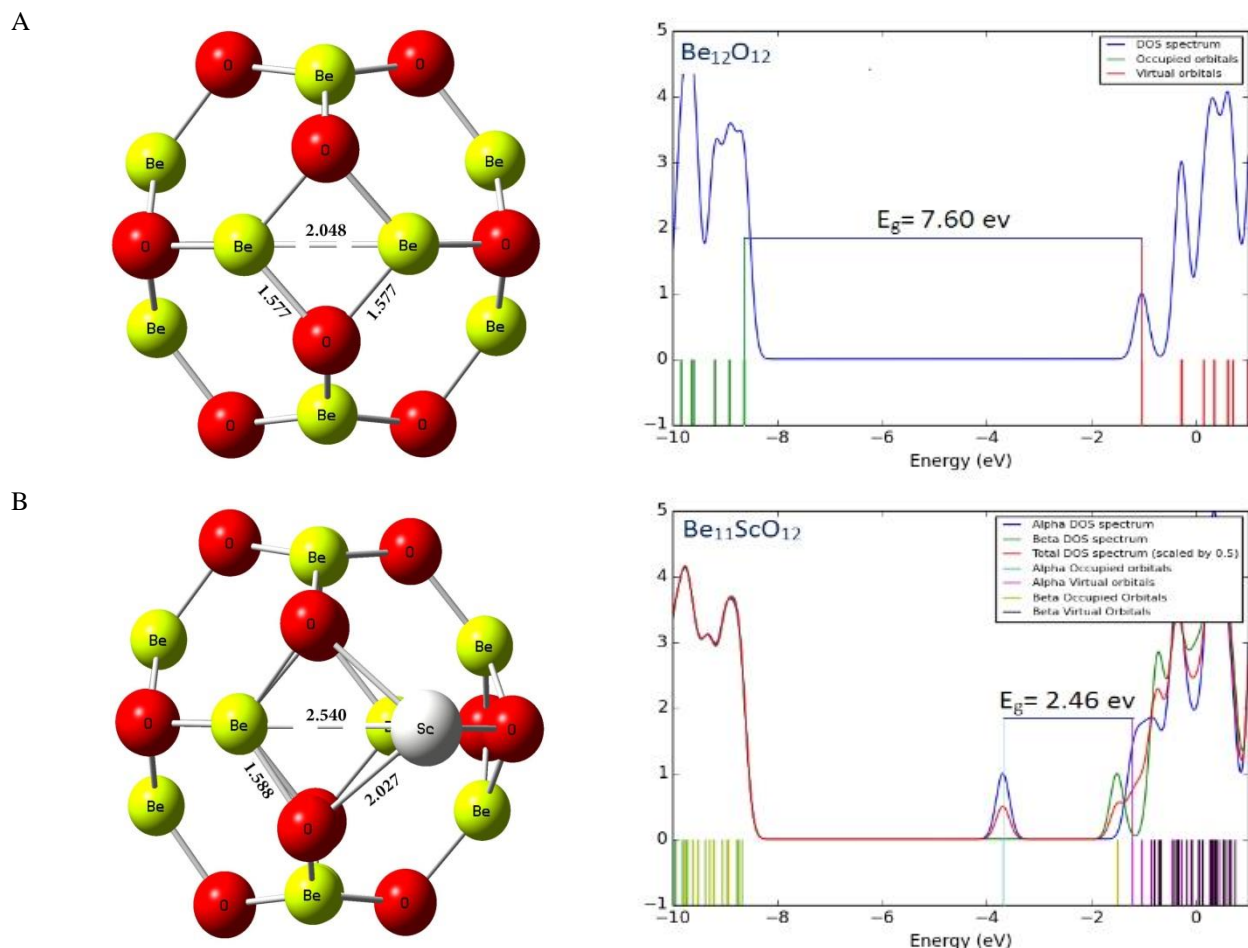
Results and Discussion

In this research, at first all structures, $\text{Be}_{12}\text{O}_{12}$ and $\text{Be}_{11}\text{XO}_{12}$ ($\text{X} =$ transition metals atom), were optimized then electronic properties, Polarizability (α) and first hyperpolarizability (β_0) $\text{Be}_{11}\text{XO}_{12}$ were studied. For all doped nano clusters ($\text{Be}_{11}\text{XO}_{12}$), calculated excitation energy was compared with the first hyperpolarizability in ground state.

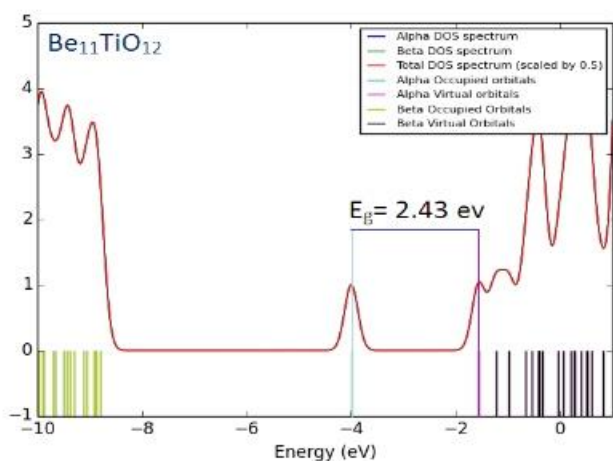
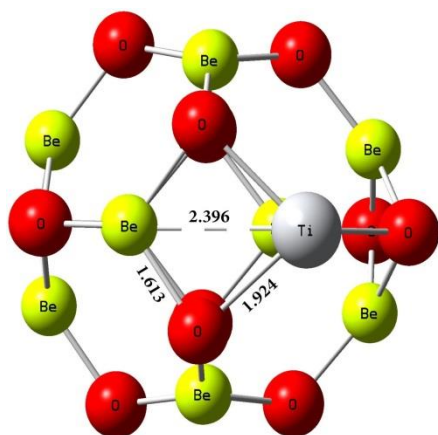
Structural and energetic investigation

All structures, $\text{Be}_{12}\text{O}_{12}$ and $\text{Be}_{11}\text{XO}_{12}$ ($\text{X} =$ transition metals atom), were optimized in the ground state by B_3LYP method and in 6-31+g(d) basis set (FIG. 1). $\text{Be}_{12}\text{O}_{12}$ nanocluster consist of square and hexagon rings that alternatively the Be atoms connected to O atoms. The Be–O and Be–Be bonds length in square ring were analyzed for pure $\text{Be}_{12}\text{O}_{12}$.

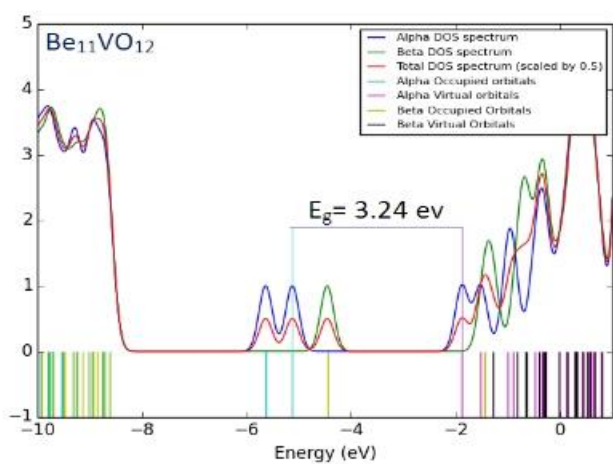
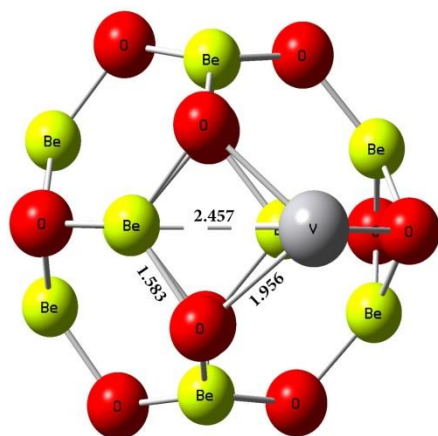
The Be–O and Be–Be bonds length were calculated and obtained 1.577 and 2.048 angstrom in pure $\text{Be}_{12}\text{O}_{12}$, respectively. Then, one of the Beryllium atoms in square ring was substituted with transition metals atom and subsequent their structures were optimized. The optimized structures of the $\text{Be}_{12}\text{O}_{12}$ and doped nanoclusters with transition metals are presented in FIG. 1.



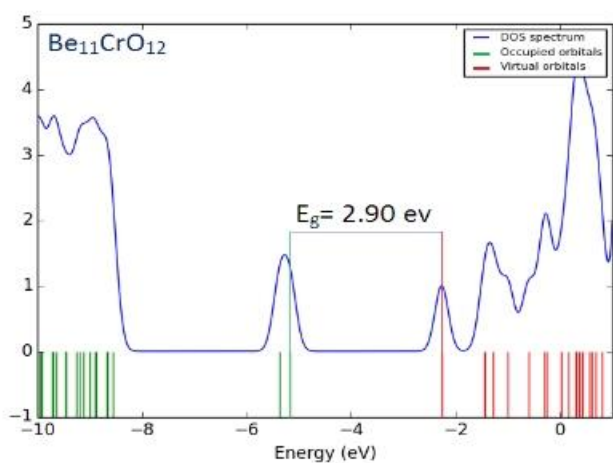
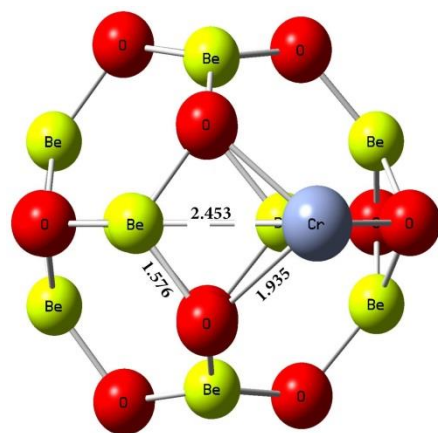
C



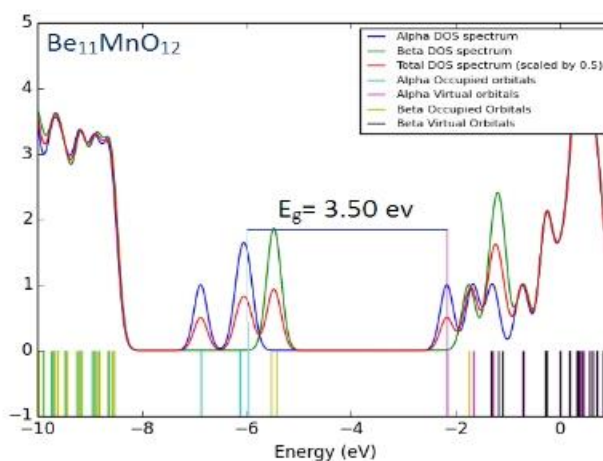
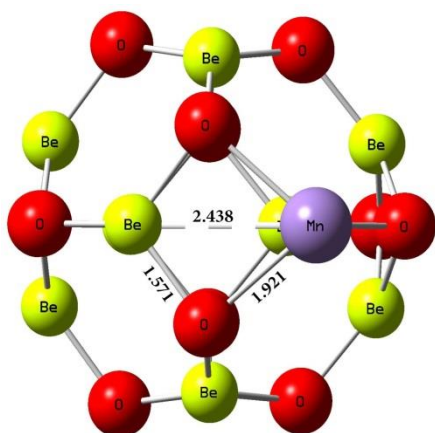
D



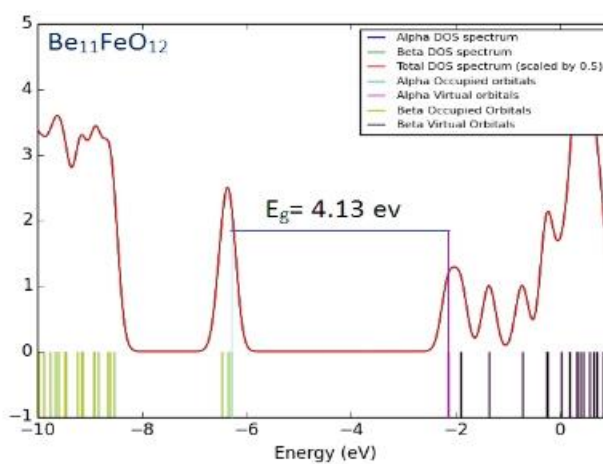
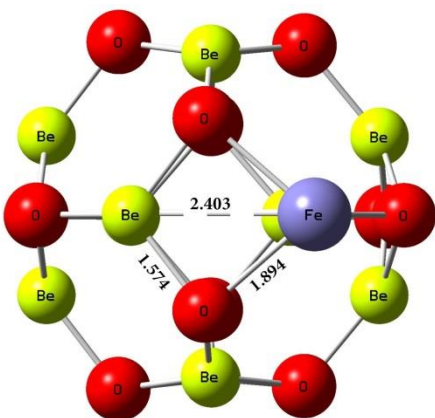
E



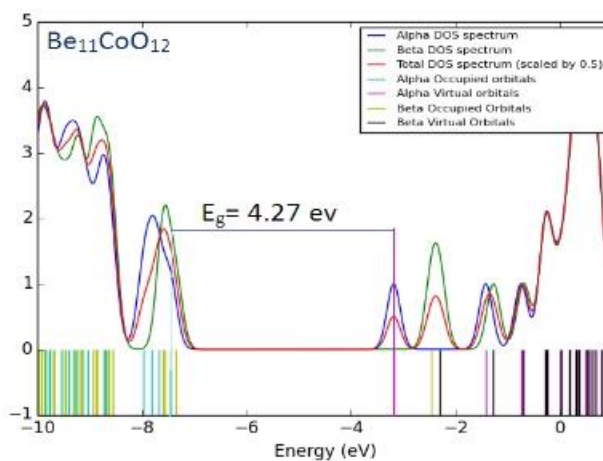
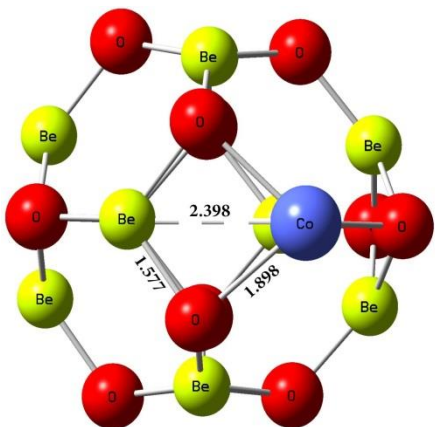
F



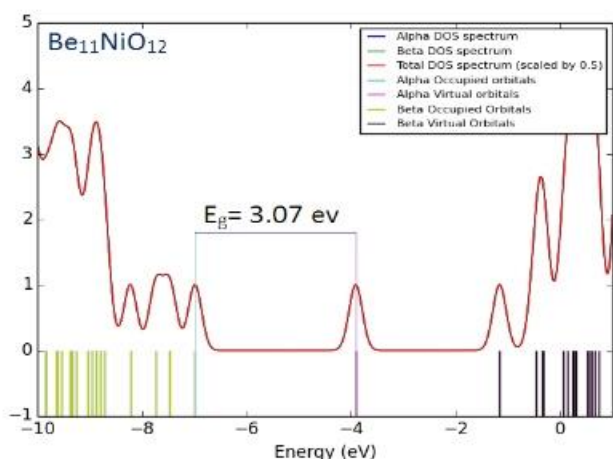
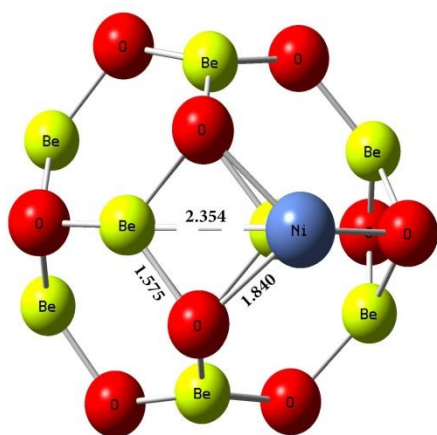
G



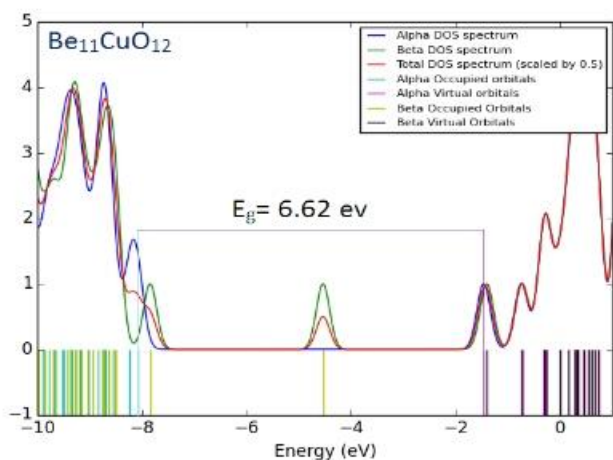
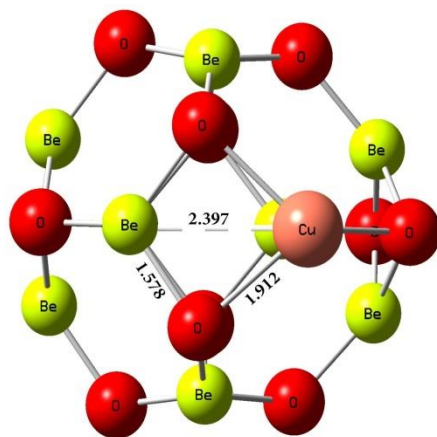
H



I



J



K

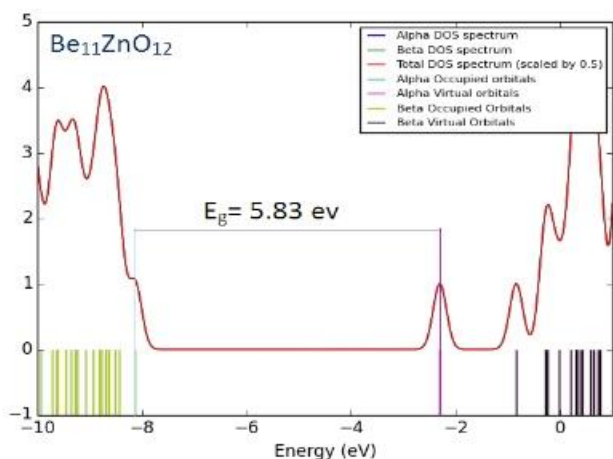
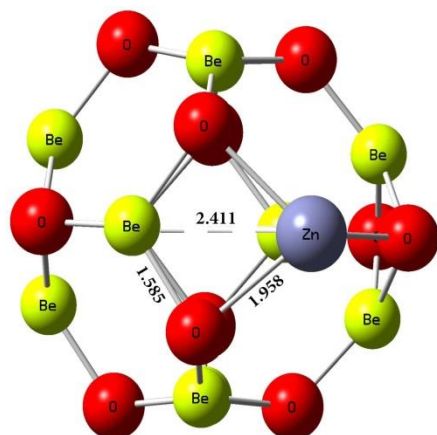


FIG. 1. The optimized geometry and density of states (DOS) spectrum of the (a) $\text{Be}_{12}\text{O}_{12}$, (b) $\text{Be}_{11}\text{ScO}_{12}$, (c) $\text{Be}_{11}\text{TiO}_{12}$, (d) $\text{Be}_{11}\text{VO}_{12}$, (e) $\text{Be}_{11}\text{CrO}_{12}$, (f) $\text{Be}_{11}\text{MnO}_{12}$, (g) $\text{Be}_{11}\text{FeO}_{12}$, (h) $\text{Be}_{11}\text{CoO}_{12}$, (i) $\text{Be}_{11}\text{NiO}_{12}$, (j) $\text{Be}_{11}\text{CuO}_{12}$ and (k) $\text{Be}_{11}\text{ZnO}_{12}$ nanocluster.

By doping transition metals atom in $\text{Be}_{12}\text{O}_{12}$ nanocluster, X-Be bond length in square ring increase and was compared to Be-Be bond length in pure $\text{Be}_{12}\text{O}_{12}$ and similar ring.

The variations maximum of bond length in among all of X-Be bonds appear for Sc-Be bond and Ni-Be bond length has the variations minimum; they were calculated 2.540 and 2.354 angstrom, respectively. Similarly, X-O bond length was increased for all doped atoms with transition metal.

The X-O, O-Be and X-Be bond length, O-X-O and O-Be-O bond angle in square ring, and doping energy for $\text{Be}_{12}\text{O}_{12}$ and doped nano cluster ($\text{Be}_{11}\text{XO}_{12}$) were gathered in TABLE. 1.

TABLE 1. X-O, O-Be and X-Be bond length (Angstrom), O-X-O and O-Be-O bond angle (degree) for square ring, $E_{\text{Be}_{11}\text{XO}_{12}}$ (Kcal mol⁻¹) and E_{dop} (Kcal mol⁻¹) for $\text{Be}_{12}\text{O}_{12}$ and other doped nano cluster ($\text{Be}_{11}\text{XO}_{12}$).

Molecule	Bond length			Bond angle		$E_{\text{Be}_{11}\text{XO}_{12}}$	E_{dop}
	X-O	O-Be	X-Be	O-X-O	O-Be-O		
$\text{Be}_{12}\text{O}_{12}$	1.577	1.578	2.048	98.211	98.199	-1.72	---
$\text{Be}_{11}\text{ScO}_{12}$	2.027	1.588	2.54	77.346	105.86	-2.91	-5.87
$\text{Be}_{11}\text{TiO}_{12}$	1.924	1.613	2.396	83.556	105.25	-3.05	-6.15
$\text{Be}_{11}\text{VO}_{12}$	1.956	1.583	2.457	79.922	105.038	-3.2	-6.46
$\text{Be}_{11}\text{CrO}_{12}$	1.935	1.576	2.453	79.777	103.827	-3.36	-6.78
$\text{Be}_{11}\text{MnO}_{12}$	1.921	1.571	2.438	80.117	103.829	-3.53	-7.12
$\text{Be}_{11}\text{FeO}_{12}$	1.894	1.574	2.403	81.719	103.841	-3.71	-7.47
$\text{Be}_{11}\text{CoO}_{12}$	1.898	1.577	2.398	81.851	104.091	-3.9	-7.85
$\text{Be}_{11}\text{NiO}_{12}$	1.84	1.575	2.354	82.745	101.078	-4.1	-8.25
$\text{Be}_{11}\text{CuO}_{12}$	1.912	1.578	2.397	88.539	104.618	-4.31	-8.68
$\text{Be}_{11}\text{ZnO}_{12}$	1.958	1.585	2.411	81.5	107.552	-4.54	-9.12

The maximum value was assigned to Sc-O bond and minimum value was calculated for Ni-O bond. Owing to TABLE. 1 Be-O bond length in $\text{Be}_{11}\text{XO}_{12}$ was shown negligible changes. The O-Be-O angle was equal to 98.2 degree. The bond angles for all of doped $\text{Be}_{12}\text{O}_{12}$ nanocluster were decreased. The minimum decrement was assigned to O-Cu-O (88.539 degree) and maximum decrement occurs at O-Sc-O (77.346 degree).

The Be-X, Be-O and Be-Be bonds length and bond angles of O-X-O for square ring, are listed in TABLE 1 and depicted in FIG. 1.

Electronic properties

The obtained DOS spectrums are shown in FIG. 1. The Obtained E_{HOMO} , E_{LUMO} and E_{g} values from DOS spectrum (FIG. 1) are listed in TABLE 2. Energy gap for $\text{Be}_{12}\text{O}_{12}$ was about 7.60 eV ($\text{Be}_{12}\text{O}_{12}$ is an intrinsic semiconductor material because of large gap bond). As can be seen in TABLE 2, substitution 1 Be atom with 1 X atom (transition metals) in $\text{Be}_{12}\text{O}_{12}$ nanocluster leads to decreasing of HOMO-LUMO energy gap (E_{g}) so that it is transformed from an intrinsic semiconductor ($E_{\text{g}} \approx 7.60$ eV) to a p-type one ($E_{\text{g}} \approx 2.43$ eV). The least of E_{g} value among all considered clusters about 2.18 eV and it belongs to $\text{Be}_{11}\text{ScO}_{12}$. The plot of E_{g} as a function of atomic number (z) indicates in FIG. 2.

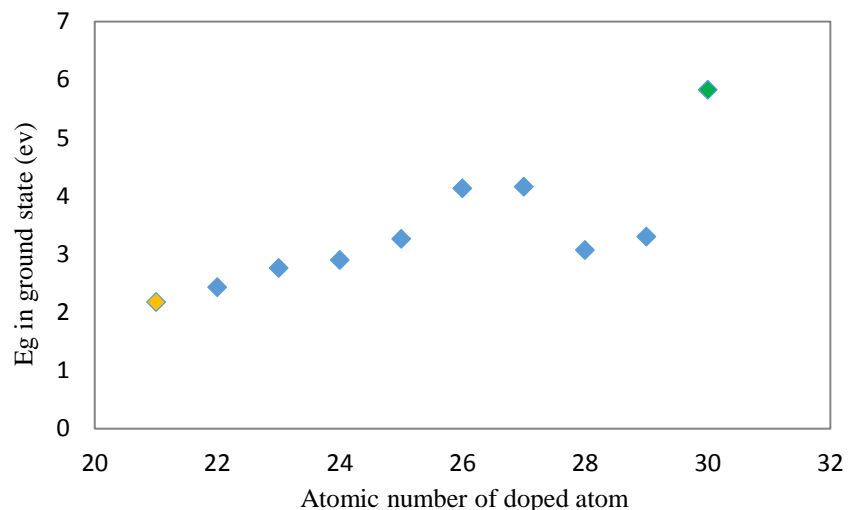


FIG. 2. The changes of energy gap (E_g) as function of atomic number of the doped transition metal atom (Z) for all considered nano clusters $Be_{11}XO_{12}$

The energy gap values for doped nanocluster $Be_{11}XO_{12}$ increase with increasing atomic number. The chemical potential of $Be_{11}XO_{12}$ was calculated and summarized in TABLE 2. The energy gap values for doped nanocluster $Be_{11}XO_{12}$ increase with increasing atomic number. The chemical potential analysis shows that doping of X atoms in $Be_{12}O_{12}$ nanocluster leads to the increasing of chemical potential. The maximum chemical potential value occurs in $Be_{11}TiO_{12}$. In FIG. 3, we can see the reduction of Chemical potential $Be_{12}O_{12}$ as a function of atomic number.

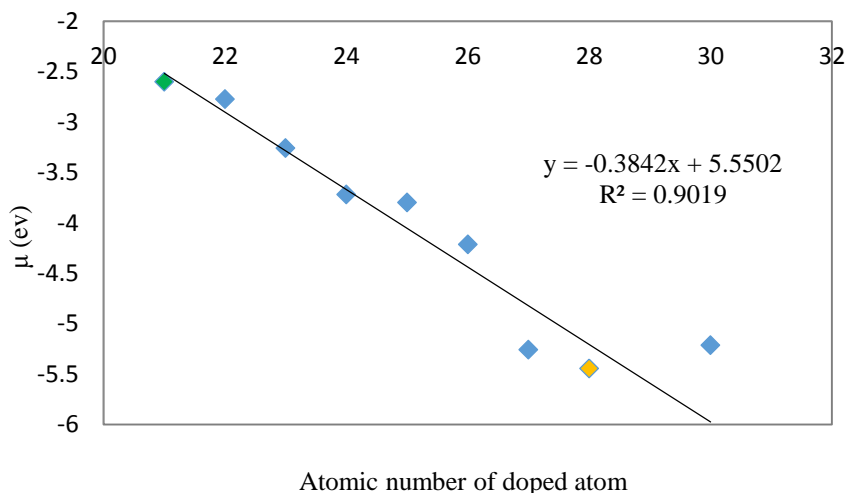


FIG. 3. Chemical potential of considered nanoclusters as function of the doped atomic number of doped transition metal atom (Z).

Optical properties

Polarizability (α) and first hyperpolarizability (β_0) for all structures were calculated and listed in TABLE. 2.

TABLE. 2. The frontier molecular orbital energies E_{HOMO} and E_{LUMO} (eV), energy gap E_g (eV), chemical potential μ (ev), percent of difference energy gap from $\text{Be}_{12}\text{O}_{12}$ $\Delta(E_{0g}-E_g)$ %, polarizability α (au) and First hyperpolarizability β^0 (au) values for the considered doped $\text{Be}_{12}\text{O}_{12}$ nanocluster.

Molecule	E_{HOMO}	E_{LUMO}	E_g	μ	$\Delta E\%$	α	β^0
$\text{Be}_{12}\text{O}_{12}$	-8.64	-1.04	7.60	0.00	0	127.55	0
$\text{Be}_{11}\text{ScO}_{12}$	-3.69	-1.51	2.18	-2.46	-71.32	187.01	4953.19
$\text{Be}_{11}\text{TiO}_{12}$	-3.99	-1.56	2.43	-2.78	-68.03	165.94	2757.35
$\text{Be}_{11}\text{VO}_{12}$	-4.64	-1.88	2.76	-3.50	-63.68	155.83	2106.40
$\text{Be}_{11}\text{CrO}_{12}$	-5.17	-2.27	2.90	-3.72	-61.84	149.31	1343.50
$\text{Be}_{11}\text{MnO}_{12}$	-5.43	-2.17	3.26	-4.07	-57.11	145.03	1069.90
$\text{Be}_{11}\text{FeO}_{12}$	-6.28	-2.15	4.13	-4.22	-45.66	142.70	777.53
$\text{Be}_{11}\text{CoO}_{12}$	-7.34	-3.18	4.16	-5.32	-45.26	139.71	348.33
$\text{Be}_{11}\text{NiO}_{12}$	-6.98	-3.91	3.07	-5.45	-59.61	138.88	166.20
$\text{Be}_{11}\text{CuO}_{12}$	-7.84	-4.54	3.30	-4.77	-56.58	139.33	248.36
$\text{Be}_{11}\text{ZnO}_{12}$	-8.13	-2.30	5.83	-5.22	-23.29	136.23	175.34

The value of 127.55 and 0 a.u. were obtained for polarizability (α) and first hyperpolarizability (β_0) of $\text{Be}_{12}\text{O}_{12}$ respectively. The results indicated that doping of transition metals atom in $\text{Be}_{12}\text{O}_{12}$ leads to increase the polarizability (α) and first hyperpolarizability (β_0) of cluster. Among all of the considered doped nanoclusters by transition metals atom, $\text{Be}_{11}\text{ScO}_{12}$ ($X=\text{Sc}$) has the largest first hyperpolarizability ($\beta_0 \approx 4953.2$ au) and polarizability ($\alpha \approx 187.01$ au) values. It was seen that by increasing the atomic number of doped transition metal the polarizability and first hyperpolarizability values was reduced (FIG. 4 and 5).

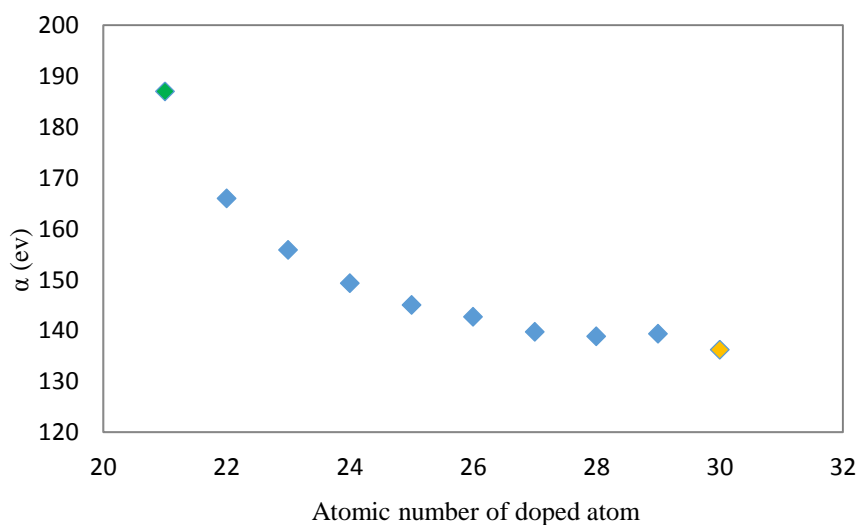


FIG. 4. The values of polarizability (α) as function of the doped transition metal atomic number (Z).

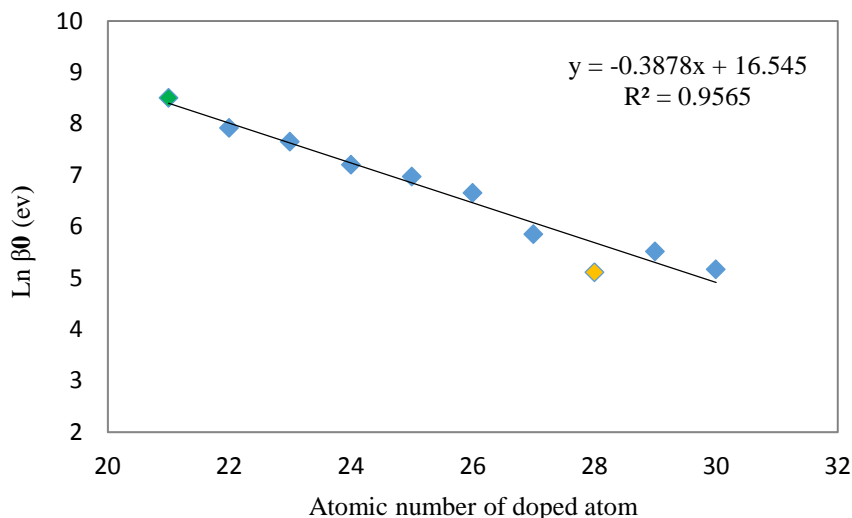


FIG. 5. Logarithmic plot of first hyperpolarizability(β_0) as a function of the doped transition metal atomic number (Z) for all considered nanoclusters.

Similar to previous research, the Sc atom doping had maximum effect on the polarizability and first hyperpolarizability of $\text{Be}_{11}\text{XO}_{12}$. Additionally, polarizability and hyperpolarizability decrease when the atomic number of transition metal increases. However larger size of $\text{Mg}_{11}\text{ScO}_{12}$ in comparison to $\text{Be}_{11}\text{ScO}_{12}$ may explain the larger value of first hyperpolarizability of $\text{Mg}_{11}\text{ScO}_{12}$.

TD-DFT calculations

To understand how doping of different transition metals effect on the β_0 values of $\text{Be}_{12}\text{O}_{12}$, the widely common two-level model is considered as [34-37]:

$$\beta_0 \propto \Delta\mu \cdot f / \Delta E^3 \quad (6)$$

where ΔE , f_0 and $\Delta\mu$ are the transition energy, oscillator strength, and difference in the dipole moments between the ground state and the crucial excited state with the largest oscillator strength. In this model, the third power of the transition energy is reversely proportional to the β_0 value; therefore the transition energy is the noteworthy factor in the first hyperpolarizability. The fraction of $\Delta\mu \cdot f / \Delta E^3$ in Eq 6, voluntary named as β_2 . The crucial transition excited state is provided using the time-dependent density functional theory (TD-DFT) calculations at CAM-B₃LYP/6-31+G(d) level of theory. The obtained values of ΔE , λ (wavelength of adsorbed light), f_0 , $\Delta\mu$ and the β_2 as well as $\ln(\beta_0)$ are presented in TABLE 3.

TABLE. 3. The first hyperpolarizability (β_0), the transition energy (ΔE), the difference of dipole moment ($\Delta\mu$) between the ground state and the crucial excited state, the largest oscillator strength (f) of the considered nanoclusters.

System	$\text{Ln } \beta$ (ev)	ΔE (ev)	λ (nm)	$\Delta\mu$ ge (a.u)	f	β_2 (a.u)
$\text{Be}_{11}\text{ScO}_{12}$	8.51	2.17	570.80	0.49	0.09	15.00
$\text{Be}_{11}\text{TiO}_{12}$	7.92	3.37	368.40	0.40	0.05	10.15
$\text{Be}_{11}\text{VO}_{12}$	7.65	3.67	337.46	0.32	0.07	9.75
$\text{Be}_{11}\text{CrO}_{12}$	7.20	4.17	297.39	0.24	0.13	8.61
$\text{Be}_{11}\text{MnO}_{12}$	6.98	4.23	292.96	0.25	0.12	7.74
$\text{Be}_{11}\text{FeO}_{12}$	6.66	4.48	276.89	0.23	0.12	6.00
$\text{Be}_{11}\text{CoO}_{12}$	5.85	5.56	214.60	0.29	0.08	2.67
$\text{Be}_{11}\text{NiO}_{12}$	5.11	6.11	202.98	0.49	0.03	1.34
$\text{Be}_{11}\text{CuO}_{12}$	5.51	4.31	287.59	0.48	0.03	4.02
$\text{Be}_{11}\text{ZnO}_{12}$	5.17	7.02	176.56	1.70	0.05	5.04

For all doped nano clusters ($\text{Be}_{11}\text{XO}_{12}$), calculated excitation energy was compared with the first hyperpolarizability obtained from TABLE 2 and was show that in the cases which have lower excitation energy, the hyperpolarizability has higher value. In FIG. 6 the simultaneously the hyperpolarizability and excitation energy of transition of doped nanocages were plotted as function of atomic number of used transition metal atoms.

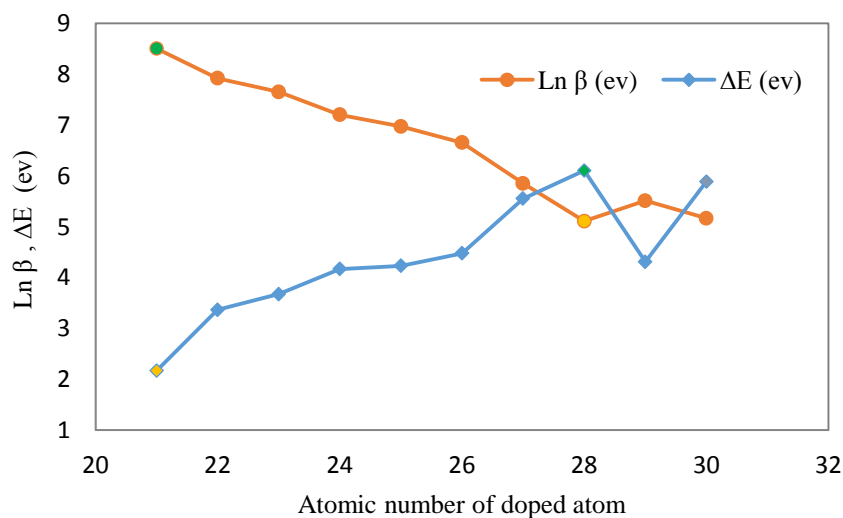


FIG. 6. The plot of first hyperpolarizability (β_0) and transition energy as function of the doped transition metal atomic number (Z) for all considered nanoclusters.

As indicated in Eq 6, the first hyperpolarizability of the doped nanoclusters is inversely proportional to the transition energies. The highest first hyperpolarizability and the lowest transition energy were observed in $\text{Be}_{11}\text{ScO}_{12}$. Additionally, the lowest first hyperpolarizability was obtained for $\text{Be}_{11}\text{NiO}_{12}$ had highest value of transition energy.

Finally, the first hyperpolarizability presented in TABLE 2, was compared with values of hyperpolarizability calculated by Eq 6. It was seen that the trend of both of them as function of atomic number of transition metals are similar. In FIG. 7, both

of the plots of logarithm of first hyperpolarizability calculated from direct ab initio calculation and the β_2 obtained from Eq 6 were plotted as function of atomic number of transition metals.

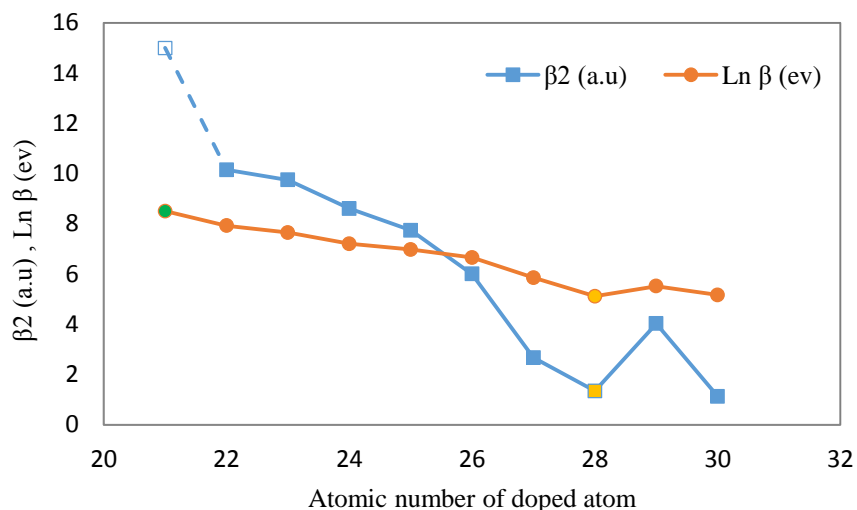


FIG. 7. Comparison between the β_0 presented in TABLE 2 and β_0 calculated by from Eq 6 (β_2).

As illustrated in FIG. 7, logarithm of first hyperpolarizability calculated by ab initio calculation has same behavior as β_0 obtained from Eq 6.

Conclusion

The aim of this study was to evaluate the effect of doping transition metals atom on the structural, electronic, linear and nonlinear optical properties of $\text{Be}_{12}\text{O}_{12}$ nanocluster by density functional theory (DFT) methods. The main conclusions of this paper can be summarized as follows:

1. Transition metals atom doping in $\text{Be}_{12}\text{O}_{12}$ nanocluster due to reduction of energy gap $\text{Be}_{12}\text{O}_{12}$. The maximum decrement belongs to $\text{Be}_{11}\text{TiO}_{12}$ (-68.03%) and the minimum decrement belongs to $\text{Be}_{11}\text{CuO}_{12}$ (-12.89%).
2. The doping of transition metals atom in $\text{Be}_{12}\text{O}_{12}$ leads to enhancement of polarizability (α). The $\text{Be}_{11}\text{ScO}_{12}$ has the greatest polarizability ($\alpha = 187.01$ eV) and $\text{Be}_{11}\text{ZnO}_{12}$ has the lowest polarizability ($\alpha = 136.23$ eV).
3. The first hyperpolarizability values increases with transition metals atom doping. The first hyperpolarizability for considered nanoclusters are change in the order of (Sc) > (Ti) > (V) > (Cr) > (Mn) > (Fe) > (Co) > (Cu) > (Ni) > (Zn).
4. The two-level model proposes that the considerable increment of β_0 is mainly due to the ΔE values. Additionally, the TD-DFT calculation indicates that the first hyperpolarizability has similar behavior as β_2 and inverse of ΔE^3 .
5. The doping process of transition metals atom in the $\text{Be}_{12}\text{O}_{12}$ nanocluster plays an important role in enhancing the first hyperpolarizability and leads to the NLO response.

REFERENCES

1. Kleinman DA. Nonlinear dielectric polarization in optical media. *Phys Rev.* 1962;126:1977.
2. Pandey V, Mehta N, Tripathi SK, et al. Optical band gap and optical constants in $\text{Se}_{85}\text{Te}_{15-x}\text{Pb}_x$ thin films. *J. Optoelectron. Adv Mater.* 2005;7:2641-6.
3. Zhong RL, Xu HL, Muhammad S, et al. The stability and nonlinear optical properties: Encapsulation of an excess electron compound $\text{LiCN}\cdots\text{Li}$ within boron nitride nanotubes. *J Mater Chem.* 2012;22:2196-202.
4. Tu C, Yu G, Yang G, et al. Constructing (super) alkali–boron-heterofullerene dyads: an effective approach to achieve large first hyperpolarizabilities and high stabilities in $\text{M}_3\text{O-BC}_{59}$ (M= Li, Na and K) and K@ n-BC_{59} (n= 5 and 6). *Phys Chem Chem Phys.* 2014;16:1597-606.
5. Zhou F, He JH, Liu Q, et al. Materials chemistry. *J Mater Chem.* 2014;100: 6850-8.
6. Hatua K, Nandi PK. Beryllium-cyclobutadiene multidecker inverse sandwiches: electronic structure and second-hyperpolarizability. *J Phys Chem A.* 2013;117:12581-9.
7. Muhammad S, Xu H, Su Z. Capturing a synergistic effect of a conical push and an inward pull in fluoro derivatives of $\text{Li@ B}_{10}\text{H}_{14}$ basket: toward a higher vertical ionization potential and nonlinear optical response. *J Phys Chem A.* 2011;115:923-31.
8. Marder SR, Gorman CB, Meyers F, et al. A unified description of linear and nonlinear polarization in organic polymethine dyes. *Science.* 1994;265:632-5.
9. Shakerzadeh E. A theoretical study on the influence of carbon and silicon doping on the structural and electronic properties of $(\text{BeO})_{12}$ nanocluster. *J Inorg Organomet Polym.* 2014;24:694-705.
10. Shakerzadeh E. A theoretical study on pristine and doped germanium carbide nanoclusters. *J Mater Sci Mater Electron.* 2014;25:4193-9.
11. Niu M, Yu G, Yang G, et al. Doping the alkali atom: an effective strategy to improve the electronic and nonlinear optical properties of the inorganic $\text{Al}_{12}\text{N}_{12}$ nanocage. *Inorg Chem.* 2013;53:349-58.
12. Iijima S. Helical microtubules of graphitic carbon. *Nature.* 1991;354:56-8.
13. Fabiański R, Firlej L, Zahab A, et al. Relationships between crystallinity, oxygen diffusion and electrical conductivity of evaporated C 70 thin films. *Solid State Sci.* 2002;4:1009-15.
14. Ma TB, Hu YZ, Wang H. Growth of ultrathin diamond-like carbon films by C_{60} cluster assembly: molecular dynamics simulations. *Diam Relat Mater.* 2009;18:88-94.
15. Jalbout AF. Endohedral metallo (80) fullerene interactions with small polar molecules. *Comput Mater Sci.* 2009;44:1065-70.
16. Lee JH, Lee BS, Au FT, et al. Vibrational and dynamic analysis of C_{60} and C_{30} fullerenes using FEM. *Comput Mater Sci.* 2012;56:131-40.
17. Jain A, Kumar V, Kawazoe Y. Ring structures of small ZnO clusters. *Comput Mater Sci.* 2006;36:258-62.
18. Beheshtian J, Bagheri Z, Kamfiroozi M, et al. A comparative study on the $\text{B}_{12}\text{N}_{12}$, $\text{Al}_{12}\text{N}_{12}$, $\text{B}_{12}\text{P}_{12}$ and $\text{Al}_{12}\text{P}_{12}$ fullerene-like cages. *J Mol Model.* 2012;18:2653-8.
19. Kakemam J, Peyghan AA. Electronic, energetic, and structural properties of C- and Si-doped $\text{Mg}_{12}\text{O}_{12}$ nano-cages. *Comput Mater Sci.* 2013;79:352-5.
20. Hong L, Wang H, Cheng J, et al. Lowest-energy structures of $(\text{MgO})_n$ (n= 2–7) clusters from a topological method and first-principles calculations. *Comput Theor Chem.* 2012;980:62-7.

21. Shakerzdeh E, Tahmasebi E, Shamlouei HR. The influence of alkali metals (Li, Na and K) interaction with $\text{Be}_{12}\text{O}_{12}$ and $\text{Mg}_{12}\text{O}_{12}$ nanoclusters on their structural, electronic and nonlinear optical properties: A theoretical study. *Synthetic Metals*. 2015;204:17-24.
22. Tahmasebi E, Shakerzadeh E, Biglari Z. Theoretical assessment of the electro-optical features of the group III nitrides ($\text{B}_{12}\text{N}_{12}$, $\text{Al}_{12}\text{N}_{12}$ and $\text{Ga}_{12}\text{N}_{12}$) and group IV carbides (C_{24} , $\text{Si}_{12}\text{C}_{12}$ and $\text{Ge}_{12}\text{C}_{12}$) nano-clusters encapsulated with alkali metals (Li, Na and K). *Appl Surf Sci*. 2016;363:197-208.
23. Shamlouei HR, Nouri A, Mohammadi A, et al. Influence of transition metal atoms doping on structural, electronic and nonlinear optical properties of $\text{Mg}_{12}\text{O}_{12}$ nanoclusters: A DFT study. *Physica E Low Dimens Syst Nanostruct*. 2016;77:48-53.
24. Frisch MJ, Trucks GW, Schlegel HB, et al. Gaussian 09, revision a. 02, Gaussian, Inc., Wallingford, CT. 2009;200.
25. Yanai T, Tew DP, Handy NC. A new hybrid exchange–correlation functional uses the Coulomb-attenuating method (CAM-B₃LYP). *Chem Phys Lett*. 2004;393(1):51-7.
26. Jacquemin D, Perpète EA, Scalmani G, et al. Assessment of the efficiency of long-range corrected functionals for some properties of large compounds. *J Chem Phys*. 2007;126:144-145.
27. Limacher PA, Mikkelsen KV, Lüthi HP. On the accurate calculation of polarizabilities and second hyperpolarizabilities of polyacetylene oligomer chains using the CAM-B₃LYP density functional. *J Chem Phys*. 2009;130:194114.
28. Janjua MR, Jamil S, Ahmad T, et al. Quantum chemical perspective of efficient NLO materials based on dipolar trans-tetraammineruthenium (II) complexes with pyridinium and thiocyanate ligands: First theoretical framework. *Comput Theor Chem*. 2014;1033:6-13.
29. O'boyle NM, Tenderholt AL, Langner KM. CCLIB: A library for package-independent computational chemistry algorithms. *J Comput Chem*. 2008;29:839-45.
30. Buckingham AD. Permanent and induced molecular moments and long-range intermolecular forces. *Adv Chem Phys*. 1967;12:107-42.
31. McLean AD, Yoshimine M. Theory of molecular polarizabilities. *J Chem Phys*. 1967;47:1927-35.
32. Thanthiriwatte KS, De Silva KN. Non-linear optical properties of novel fluorenyl derivatives—ab initio quantum chemical calculations. *J Mol Struct Theochem*. 2002;617:169-75.
33. Wang JJ, Zhou ZJ, Bai Y, et al. The interaction between super-alkalis (M_3O , $\text{M} = \text{Na}, \text{K}$) and a $\text{C}_{20}\text{F}_{20}$ cage forming superalkali electride salt molecules with excess electrons inside the $\text{C}_{20}\text{F}_{20}$ cage: dramatic superalkali effect on the nonlinear optical property. *J Mater Chem*, 2012;22:9652-7.
34. Oudar JL, Chemla DS. Hyperpolarizabilities of the nitroanilines and their relations to the excited state dipole moment. *J Chem Phys*. 1977;66:2664-8.
35. Oudar JD. Optical non-linearities of conjugated molecules. Stilbene derivatives and highly polar aromatic compounds. *J Chem Phys*. 1977;67:446-57.
36. Kanis DR, Ratner MA, Marks TJ. Design and construction of molecular assemblies with large second-order optical nonlinearities. Quantum chemical aspects. *Chem Rev*. 1994;94:195-242.
37. Datta A, Pati SK. Dipolar interactions and hydrogen bonding in supramolecular aggregates: understanding cooperative phenomena for 1st hyperpolarizability. *Chem Soc Rev*. 2006;35:1305-23.